THE JOURNAL OF BIOLOGICAL CHEMISTRY
Vol. 274, No. 49, Issue of December 3, pp. 34916–34923, 1999

Printed in U.S.A.

Territrem B, a Tremorgenic Mycotoxin That Inhibits Acetylcholinesterase with a Noncovalent yet Irreversible Binding Mechanism*

(Received for publication, June 30, 1999)

Jen-Wei Chen‡, Ying-Ling Luo§¶, Ming-Jing Hwang¶‖, Fu-Chuo Peng§, and Kuo-Huang Ling‡‖

From the ‡Institute of Biochemistry and §Institute of Toxicology, College of Medicine, National Taiwan University, Taipei, 100 Taiwan and ¶Division of Structural Biology, Institute of Biomedical Sciences, Academia Sinica, Taipei, 115 Taiwan

Territrem B (TRB) is a fungal metabolite isolated from *Aspergillus terreus* shown previously to be a potent and irreversible inhibitor of acetylcholinesterase (AChE). In the present study, a number of binding and inhibition assays were carried out to further characterize the inhibitory effect of TRB. The results indicate that the binding of TRB (*a*) is much more selective than a well characterized selective inhibitor of AChE, BW284C51, (*b*) adopts a one-to-one stoichiometry with the enzyme, (*c*) cannot be undone by an AChE-regenerating oxime agent, which contrasts the ability of 8 M urea to release AChE-bound TRB, (*d*) is enhanced by high concentration NaCl but prevented, unless preincubated, by Triton X-100, and (*e*) exhibits quasi-first order kinetics with an overall inhibition constant of 0.01 nM^{-1} min^{-1}. Together these results suggest a very different irreversible binding (a noncovalent type) from that of the covalent type, which involves typical irreversible AChE inhibitors such as diisopropylfluorophosphate and neostigmine. According to the prediction of a molecular modeling study, the distinct AChE inhibitory characteristics of TRB may arise from the inhibitor being noncovalently trapped within a unique active-site gorge structure of the enzyme. It was predicted that an optimal TRB·AChE binding would position a narrowing connection of the TRB structure at a constricted area near the entrance of the gorge, thereby providing a structural basis for the observed irreversible binding.

The termination of impulse transmission at cholinergic synapses is enabled by acetylcholinesterase (AChE[1]; EC 3.1.1.7), a highly efficient enzyme capable of hydrolyzing its substrate by a turnover rate of 10^4 s^{-1} (1, 2). An unusual feature revealed by the crystal structure of this enzyme (3) is that its catalytic center is buried at the bottom of a narrow gorge approximately 20 Å in length. Instead of illuminating, this gorge structure further mystifies the mechanism of the catalytic power of AChE and consequently inspires intriguing hypotheses from a number of theoretical investigations (4–8). On the other hand, the long and narrow substrate passage and multiple reaction subsites provide ample places upon which inhibitors may act, which helps explain the fact that a structurally diverse set of compounds can inhibit AChE with differing inhibitory kinetics and action mechanisms (9).

There are two major types of AChE inhibitors (9, 10): (*a*) those that inactivate the enzyme by carbamoylating or phosphorylating the catalytic serine (the inhibition of this type is irreversible, but regeneration of the enzyme activity can be achieved via deacetylation (*e.g.* using an agent such as pyridine-2-aldoxime methiodide, 2-PAM)) and (*b*) those that inactivate the enzyme by blocking the access of the substrate to the active center and/or by inducing defective conformational change of the enzyme with noncovalent binding (the inhibition of this type is reversible). Both types of AChE inhibitors are current targets of drug development for treating Alzheimer's disease (10).

About three decades ago, Ling and co-workers (52) found that the stored unhulled rice of Taiwan was heavily polluted by the three major groups of fungi—*Aspergillus*, *Penicillium*, and *Rhizopus*. A family of fungal metabolites was subsequently isolated from the chloroform extracts of submerged rice culture of *Aspergillus terreus* 23-1. These fungal metabolites were given the name "territrem" to indicate their biological origin of *A. terreus* and the tremorgenic activities they induced in rat and mice (reviewed in Ref. 11). In an experiment with the central neuron of the snail *Achatinae fatice*, it was further found that territrem B (TRB) potentiates the acetylcholine-induced current of the neuron but has no effect on γ-aminobutyric acid - or L-glutamate-elicited currents (12). These results suggested that the tremorgenic effects of territrems arise from their being a potent inhibitor of AChE. This suggestion was first supported by the observed inhibitory activities of territrems on AChE extracted from the head of an insect (13). More recently, TRB and other members of the territrem family were shown to bind tightly and inhibit irreversibly eel AChE with an IC_{50} value in the order of 10^{-8} M (14). Independently, Omura *et al.* (15) confirmed that territrems are potent AChE inhibitors by reporting the inhibitory activities of TRB and territrem C (TRC) on AChE from human erythrocytes. Omura's group additionally showed that several analogs of territrem isolated from rice culture broth of *Penicillium* sp. FO-4259, which the researchers called arisugacins, are highly specific and potent AChE inhibitors as well (15, 16). Both territrems and arisugacins are composed of a basic structure that includes a benzyl group, a pyran, and a terpenoid (Fig. 1). The notable absence of nitrogen in these compounds, as in onchidal (18), is unlike other known AChE inhibitors.

* This work was supported by National Science Council Grants 85-0412-B-002-026 Z and 86-2621-B-002-022 B. The costs of publication of this article were defrayed in part by the payment of page charges. This article must therefore be hereby marked "*advertisement*" in accordance with 18 U.S.C. Section 1734 solely to indicate this fact.

‖ To whom reprint requests and correspondence concerning molecular modeling should be addressed (to M.-J. H.): Institute of Biomedical Sciences, Academia Sinica, 128 Yen-chiou Yuan Rd, Sec. 2, Taipei 115, Taiwan. Tel.: 886-2-2789-9033; Fax: 886-2-2788-7641; E-mail: mjhwang@ibms.sinica.edu.tw. Correspondence concerning biochemical experiments should be addressed to K.-H. L.

[1] The abbreviations used are: AChE, acetylcholinesterase; BChE, butyrylcholinesterase; TRB, territrem B; TRC, territrem C; 2-PAM, pyridine-2-aldoxime methiodide; DFP, diisopropylfluorophosphate; BW284C51, 1,5-bis(4-allyldimethylammoniumphenyl)pentan-3-one dibromide; E2020, (*R*,*S*)-1-benzyl-4-[(5,6-dimethoxy-1-indanon)-2-yl] methylpiperidine; hupA, huperzine A.

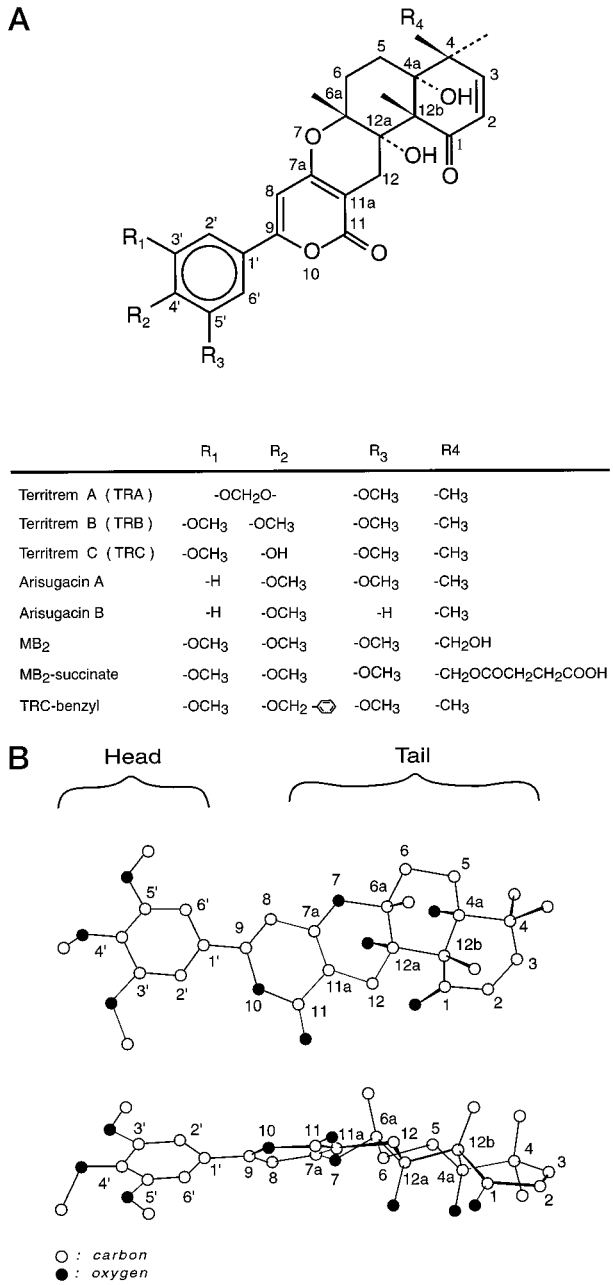

	R_1	R_2	R_3	R4
Territrem A (TRA)	$-OCH_2O-$		$-OCH_3$	$-CH_3$
Territrem B (TRB)	$-OCH_3$	$-OCH_3$	$-OCH_3$	$-CH_3$
Territrem C (TRC)	$-OCH_3$	-OH	$-OCH_3$	$-CH_3$
Arisugacin A	-H	$-OCH_3$	$-OCH_3$	$-CH_3$
Arisugacin B	-H	$-OCH_3$	-H	$-CH_3$
MB_2	$-OCH_3$	$-OCH_3$	$-OCH_3$	$-CH_2OH$
MB_2-succinate	$-OCH_3$	$-OCH_3$	$-OCH_3$	$-CH_2OCOCH_2CH_2COOH$
TRC-benzyl	$-OCH_3$	$-OCH_2$-	$-OCH_3$	$-CH_3$

FIG. 1. **The territrem family.** *A,* structure of some territrems and their derivatives. MB_2 is a major metabolyte of TRB isolated from rat liver microsomal fraction (17). *B,* two views of the TRB molecule.

In the present study, we investigated the mechanism of TRB AChE inhibition using both kinetic and molecular modeling studies. Our data indicate that TRB does not form a covalent bond with the enzyme. This result is counterintuitive. One would expect the opposite due to the irreversibility of the inhibition. However, the finding that TRB does not form a covalent bond with the enzyme is consistent with its lack of a carbamate and a phosphate moiety, which could otherwise react with the active serine of the enzyme. By searching for a probable binding mode between TRB and AChE through extensive docking simulations, a structural model of their complex was derived. This model appears to explain the novel noncovalent yet irreversible AChE-inhibiting mechanism of TRB.

EXPERIMENTAL PROCEDURES

Materials—A. terreus 23-1 was cultivated, and TRB was isolated as described by Ling *et al.* (19, 20). TRB with a purity greater than 99.5% was achieved by two-dimensional TLC (21) and high performance liquid chromatography (22). The concentration of TRB in methanol was determined spectrophotometrically and calculated from the molar absorption coefficient of 18,400 at 331 nm in methanol (23). [^{14}C]TRB was synthesized from TRC and [^{14}C]dimethylsulfate (24). Acetylthiocholine iodide, butyrylthiocholine iodide, neostigmine bromide, 1,5-bis(4-allyldimethylammoniumphenyl)pentan-3-one dibromide (BW284C51), 5,5′-dithiobis(2-nitrobenzoic acid), and bovine serum albumin were purchased from Sigma. Diisopropylfluorophosphate (DFP) and Triton X-100 were obtained from Merck. Sephadex G-50 (fine) was purchased from Amersham Pharmacia Biotech. 2,5-Diphenyloxazole, 1,4-bis-2-(5-phenyloxazolyl)benzene, and [^{14}C]dimethylsulfate (11.5 mCi/mmol) were from NEN Life Science Products. Electric eel AChE (1000–12,000 units/mg of protein) and horse serum butyrylcholinesterase (BChE, 100–150 units/mg of protein) were purchased from Sigma.

Preparation of the Working Solutions of Inhibitors—The stock solutions of TRB and of neostigmine were prepared in methanol. Before use, these stock solutions were diluted with 0.1 M phosphate buffer, pH 7.0, until the content of methanol was about 10% in the working solutions. The final content of methanol in the assay was less than 1%. This content of methanol had no effect on the enzyme activity assayed, either for AChE or for BChE. The stock solution of BW284C51 was prepared by dissolving in 0.1 M phosphate buffer, pH 7.0, without the aid of methanol. The stock solution of DFP was prepared by dissolving in isopropanol to make a 0.2×10^{-3} M solution.

Assay of Enzyme Activity—A package of 1000 units of eel AChE or horse serum BChE was dissolved in 200 ml 0.1 M phosphate buffer, pH 7.0, to produce the working solution of AChE or BChE, respectively. In the experiment with NaCl or Triton X-100, the working enzyme solution contained 1 M NaCl or 1% Triton X-100. Enzyme activity was determined as described previously (14) and according to the colorimetric method of Ellman *et al.* (25). The concentration of the catalytic subunit of AChE in the working enzyme solution was calculated using a molar catalytic efficiency of 6.0×10^5 M acetylthiocholine hydrolyzed/min at 25 °C (26). The protein concentration was determined by the method of Lowry *et al.* (27). The same procedures were followed for the experiment with BChE, except that the substrate used was butyrylthiocholine and the enzyme used was horse serum BChE. Other specifics of the individual inhibition studies are separately described below.

Gel Filtration—A Sephadex G-50 column (0.5 × 25 cm) was equilibrated with 0.1 M phosphate buffer, pH 7.0, and eluted with the same buffer after application of the sample. Each 0.5-ml of effluent was collected at a flow rate of 1 ml/min.

Determination of Radioactivity—For an aqueous sample, the mixture was a mixture of toluene, Triton X-100 (1:1 by volume) containing 0.8% 2,5-diphenyloxazole and 0.02% 1,4-bis-2-(5-phenyloxazolyl)benzene (28). The radioactivity was counted with a Packard liquid scintillation analyzer, model 2200 CA.

The Progressive Inhibition of AChE by TRB—5 μl of various concentrations of TRB (40–33 nM in 10% methanol solution) were added to each 45 μl of the AChE working solution (6 nM of catalytic subunit) and then preincubated at 25 °C. At different time points during preincubation, 3 ml of the AChE assay solution was introduced, and the initial rate of substrate hydrolysis was measured. The results were analyzed by the method of Kitz and Wilson (29).

Stoichiometric Relationship of the Binding and Inhibition of AChE by [^{14}C]TRB—Each 40 μl of AChE (1.25 μM of catalytic subunit) was incubated with 40 μl of [^{14}C]TRB (0–2.5 μM dissolved in 0.1 M phosphate buffer at pH 7.0). After 1 h of incubation, an aliquot (60 μl) of the incubation mixture was applied to a G-50 column for gel filtration analysis. Each 0.5 ml of effluent was analyzed by scintillation counting. The total counts that appeared in the fractions 3 and 4, where AChE activity was found, were regarded as bound [^{14}C]TRB. The concentration of the bound [^{14}C]TRB was calculated from its specific activity (4.5 Ci/mol). To assay AChE activity, another aliquot (20 μl) of a 100-fold diluted solution of the above incubation mixture was used. The percent of AChE inhibition was determined by comparing the enzyme activity determined in the presence of TRB to that determined in the absence of TRB.

Regeneration of TRB- or DFP-inhibited AChE Activity by 2-PAM—AChE (the working enzyme solution) was incubated with either 2×10^{-5} M DFP or 1.5×10^{-8} M TRB in 0.1 M phosphate buffer, pH 7.0, until more than 99% of the AChE activity was inhibited. At 80 min after the addition of DFP or TRB, the inhibited enzyme was allowed to incubate with 2-PAM (0.04 M at the incubation). At different periods of incubation, 20-μl aliquots were removed for determination of AChE activity. The ratio of enzyme activity relative to control (*i.e.* activity measured in the absence of TRB inhibition) was determined.

Effect of Urea on the Binding of [^{14}C]TRB to AChE—Three specimens

(A, B, and C) were made as follows. Specimen A had 25 μl of 1 μM [^{14}C]TRB, 25 μl of bovine serum albumin (0.4 mg), and 50 μl of 0.1 M phosphate buffer of pH 7.0. The content of specimen B was the same as that of specimen A, except that the 50 μl of 0.1 M phosphate buffer was replaced by 50 μl of 1.25 μM AChE in 0.1 M phosphate buffer, such that the molar ratio of AChE subunit to [^{14}C]TRB was 2.5:1. Specimen C had the same content as that of specimen B plus 72 mg of urea. Specimens A and B were applied separately on different G-50 columns for gel filtration analyses. Specimen C was applied on another G-50 column previously equilibrated with a 0.1 M phosphate buffer of pH 7.0 containing 8 M urea and was then eluted with the same solvent used in equilibration. Each 0.5 ml of the effluent was collected for determination of the absorbance at 280 nm, radioactivity, and AChE activity.

Inhibition of AChE and BChE by TRB and BW284C51—Preincubation of aliquots (2.97 ml each) of the working enzyme solution of eel AChE or horse serum BChE with 30 μl of different concentrations of TRB or BW284C51 was carried out for 20 min at 25 °C. The enzyme assay was then performed by adding a mixture of 100 μl of 5,5′-dithiobis(2-nitrobenzoic acid) and 20 μl of acetylthiocholine or butyrylthiocholine to the aliquot. The enzyme activity of an experimental control, which contained the same components as the test solution except that the inhibitor was replaced with an equal amount of methanol, was regarded as 100% activity. By comparison to 100% activity of the control assay, the percent of enzyme inhibition for the inhibitor-containing solution was deduced.

Inhibition of AChE by TRB or Neostigmine in the Presence of a High Concentration of NaCl—TRB (10^{-6} M in methanol) and neostigmine (10^{-5} M in a 0.1 M phosphate buffer, pH 7.0) were diluted 10-fold with 0.1 M phosphate buffer, pH 7.0, or with the same buffer containing 1 M NaCl. An aliquot (180 μl) of the AChE working solution prepared in 0.1 M phosphate buffer, pH 7.0, or in the same buffer containing 1 M NaCl was allowed to incubate with 20 μl of either TRB or neostigmine at 25 °C. At the indicated time of incubation, 20 μl of the above mixture was sampled for AChE activity assay.

Inhibition of AChE by TRB or Neostigmine in the Presence of Triton X-100—The experimental procedures were the same as those described in the experiment with NaCl, except that 1% Triton X-100 was present in the buffer instead of NaCl. An additional experiment was carried out as follows. A solution of AChE and TRB was incubated in the absence of Triton X-100 as described above. At 12 min after incubation, the incubation mixture was diluted 2-fold to form a solution containing 1% Triton X-100. At the indicated time of further incubation, 40 μl of the 2-fold-diluted mixture was added to the assay solution for determination of AChE activity.

Molecular Modeling—The structure of TRB, as determined by x-ray (30), is rather thin and long (Fig. 1*B*). Our modeling began with an alignment of the long axis of TRB with that of the gorge of AChE (Protein Data Bank code 2ace (31)) and superimposing the respective geometric centers of the two. The gorge axis was defined by connecting the geometric center of Phe-448 side chain with the midpoint between Phe-330 and Tyr-121. This axis is not identical but is close to the one used by others (32). A total of 3024 ($14 \times 12 \times 9 \times 2$) initial AChE·TRB complex structures were then generated by translating and rotating TRB along the aligned axis by increments of 1 Å (spanning for 14 Å) and 30°, respectively, and accounting for the internal rotation of the benzyl group (every 45° starting from 0°, plus the original orientation, 14°, of the x-ray structure) as well as both directions of TRB insertion into the gorge (*i.e.* head in or tail in, with the benzyl group representing head, see Fig. 1*B*). Each of the 3024 structures was energy-minimized, and the 200 lowest interaction energy structures were roughly clustered into 20 groups (10 each, respectively, for the head-in and the tail-in insertion) of significantly dissimilar rotational orientations and axial positions of the ligand. The lowest energy structure in each of the 20 groups was then subjected to a 30-ps molecular dynamics-simulated annealing using temperatures up to 1000 K to surmount some conformational barriers. The molecular dynamics simulation, during which backbone atoms of the protein were fixed at their crystallographic coordinates, was followed by energy minimization without constraints. The resulting structures were assessed by (*a*) interaction energy between TRB and AChE, (*b*) side chain conformations of gorge residues as checked by PROCHECK (33), (*c*) root mean square deviations from the x-ray structure for both TRB and AChE, and (*d*) ability to interpret results of biochemical experiments (see "Discussion"). Based on these assessments, a TRB tail-in structure, which coincidentally was also the one that had the lowest AChE·TRB interaction energy among all, was selected as the most probable model for the binding of TRB with AChE. This binding mode was then used to generate the initial complex structure for an additional 30-ps molecular dynamics simulation at 300 K, in which the enzyme was reverted to its crystal (2ace) coordinates at the beginning of the simulation. The purpose of this additional run was to remove large conformational changes of the protein side chain (as compared with the x-ray structure), which are results of high temperature dynamics. The final structure (described below) is the resultant complex structure of this additional run, with its energy minimized.

To test the validity of these docking procedures, they were applied to predict the binding mode of (−)-huperzine A (hupA) with AChE, which is crystallographically known (protein data bank code 1vot (34)). The complex with the lowest interaction energy emerged from simulations of 720 initial structures ($15 \times 12 \times 4$ hupA configurations; 2 axes of hupA, but no internal rotation, were considered) reproduced the x-ray structure remarkably well (0.4-Å root mean square deviations for hupA upon superposition of the protein backbone). A comparison to its initially assigned configuration showed that hupA of this predicted structure was translated by 4.8 Å and rotated by 109° and 46° (respectively, for the two axes considered) during the simulation.

The InsightII/Discover program of Molecular Simulation Inc. (San Diego, California) and its consistent valence force field were employed for energy calculations and structural manipulations. The molecular dynamics simulations were proceeded with a time step of 1 fs, and 1000 steps of conjugate gradient optimization were used for energy minimization. Noncovalent interactions were calculated using a cell multiple method (35) and a distance-dependent dielectric constant ($\epsilon(r) = r$).

RESULTS

Kinetic Parameters for TRB Inhibition of AChE—To derive a kinetic model for the inhibition of TRB on AChE, enzyme activity was measured against preincubation time. The results, shown in Fig. 2*A* in a semilogarithmic plot, exhibited linearly declining lines indicative of an inhibitory mechanism of quasi-first order. Furthermore, the absence of a gradually approaching steady state in the inhibition of TRB (Fig. 2*A*) indicated no spontaneous regeneration of free enzymes. A double reciprocal plot yielded a straight line that did not pass through the origin (Fig. 2*B*), suggesting that a reversible AChE·TRB complex (EI) was present before the formation of an irreversible AChE·TRB complex (EI′) (29). Such an inhibition scheme can be illustrated in the following equation.

$$E + I \underset{}{\overset{k_d}{\longleftrightarrow}} EI \xrightarrow{k_{inact}} EI' \qquad \text{(Eq. 1)}$$

where k_d is the dissociation constant of EI, and k_{inact} is the rate constant of the formation of the inactivated complex EI′. The values of k_d and k_{inact} calculated from the intercepts of the $1/K_{app}$ *versus* 1/[I] plot (Fig. 2*B*) were 5 nM and 0.05 min^{-1}, respectively. The rate constant for the overall inhibition (k_i), as calculated from the equation $k_i = k_{inact}/k_d$, was 0.01 nM^{-1} min^{-1}.

The Nature of TRB Binding with AChE—Because the inhibition of TRB on AChE is irreversible, the molar ratio between TRB and AChE in regard to their binding and the resulting inhibition can be measured. As shown in Fig. 3, both the binding and the inhibition of [^{14}C]TRB to AChE increased linearly with increasing concentration of [^{14}C]TRB, and the highest level of binding and inhibition was observed when the concentration of [^{14}C]TRB was close to 1.25 μM, which was also the concentration of AChE added in each sample. Moreover, this highest level of inhibition and binding remained unchanged despite further increases of [^{14}C]TRB in the sample. These results indicated that one molecule of TRB binds one catalytic unit of AChE and that this binding is directly related to TRB inhibition of AChE.

The nature of the binding between TRB and AChE was further elucidated by the following. (*a*) The AChE-inhibiting time course of TRB was similar to that of DFP; however, DFP-inhibited AChE was reactivated by 2-PAM, but TRB-inhibited AChE was not (Fig. 4). (*b*) A high NaCl concentration enhanced the inhibitory effect of TRB but reduced that of

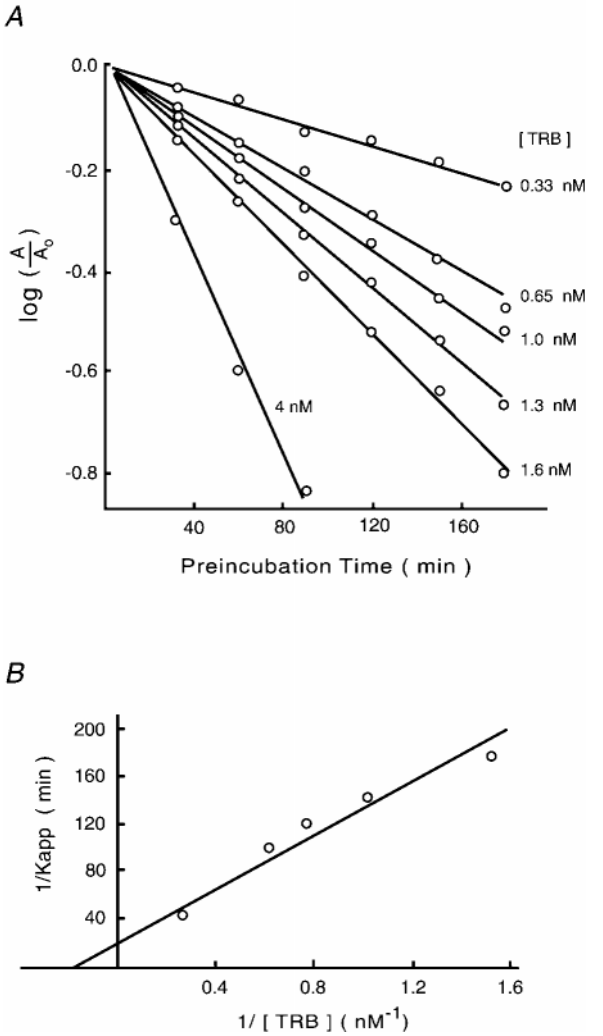

FIG. 2. **Progressive inhibition of eel AChE by TRB.** *A*, a semilogarithmic plot of the percent of the remaining enzyme activity (A/A_o, with A_o denoting the enzyme activity measured in the absence of TRB inhibition) against preincubation time. *B*, a double-reciprocal plot of rate constants against TRB concentration. The inverse of the apparent first order rate constant (K_{app}) for the inhibition of AChE activity obtained from *A* is shown *versus* the reciprocal concentration of TRB. The concentration of TRB in the figure is the final concentration at the indicated preincubation time.

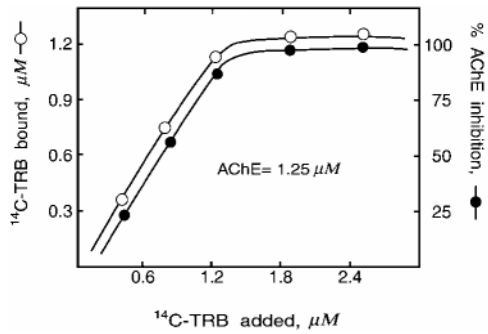

FIG. 3. **Stoichiometric relationship of the binding and inhibition of eel AChE by [^{14}C]TRB.** Various concentrations (0–2.5 μM) of [^{14}C]TRB were incubated with AChE solution (1.25 μM catalytic unit) for 1 h before aliquots of the incubation mixture were assayed for [^{14}C]TRB binding and inhibition of AChE. The concentration of the bound [^{14}C]TRB was determined by scintillation analysis using a specific activity of 4.5 Ci/mol. The percent of the remaining enzyme activity of the [^{14}C]TRB-incubated solution was determined by comparing to the activity measured for a control experiment in which no TRB was present in the solution.

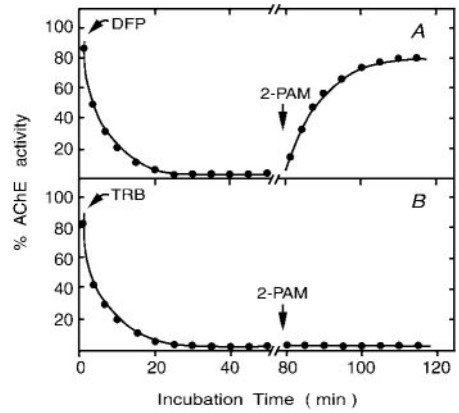

FIG. 4. **Regeneration of DFP- or TRB-inhibited eel AChE by 2-PAM.** *A*, the working enzyme solution of AChE was incubated with 2×10^{-5} M DFP. At indicated incubation times, enzyme activity was determined. *B*, same as *A* except that TRB was used as the inhibitor. An *arrow* marks the incubation time when 0.04 M 2-PAM was added to the incubation mixture.

neostigmine (Fig. 5). In comparison, preincubation with 1% Triton X-100 abrogated the inhibitory effect of TRB, whereas it had no effect on the inhibition of neostigmine. Interestingly, post-addition of Triton X-100 to TRB-inhibited AChE was unable to restore the activity of the enzyme (Fig. 6). (*c*) The binding of [^{14}C]TRB to AChE was specific (Fig. 7, *A* and *B*) and, moreover, was noncovalent because AChE-bound [^{14}C]TRB was released by treatment with 8 M urea (Fig. 7*C*). Thus, TRB inhibits AChE via a noncovalent binding mechanism, which is different from the covalent binding mechanisms of the typical irreversible inhibitors of the enzyme.

Selective Inhibition of TRB on AChE over BChE—As the inhibition experiment shown in Fig. 8 indicated, AChE was completely inhibited by 10^{-8} M TRB; in contrast, BChE was not inhibited by TRB even when the TRB concentration was increased to 10^{-3} M. A higher concentration of TRB was not tested because of its lack of further solubility. Under the same assay condition, 10^{-7} M BW284C51 completely inhibited AChE. This same concentration of BW284C51 had no inhibitory effect on BChE, but as the concentration of BW284C51 increased, it started to inhibit BChE, and at 10^{-2} M, the inhibition was essentially complete. TRB is, therefore, superior to BW284C51 in selectively inhibiting eel AChE over horse serum BChE. Consistent with this finding, the inhibitory activities of TRB and also of TRC and arisugacin A and B against horse serum BChE are several thousand times weaker than against human erythrocyte AChE (15, 16).

The Predicted AChE·TRB Binding Mode—To gain insight into the inhibitory mechanism of TRB, we determined the interaction of TRB with the AChE substrate channel (the gorge) by molecular modeling. The model predicted that TRB would bind to AChE by occupying a large portion of the gorge, making contact interactions (defined as distance < 5 Å between any pair of heavy atoms) with 23 amino acids (Fig. 9*A*). In this binding mode, TRB interacted substantially with the peripheral anionic site (Tyr-70, Asp-72, Tyr-121, Trp-279, Tyr-334) and part (Tyr-70, Asp-72, Glu-73, Gln-74, Ser-81, Trp-84, Asn-85) of a cysteine loop (Cys-69—Cys-96) that is a common structural feature of many lipases and esterases (36, 37). To a lesser extent, TRB also interacted with the oxyanion hole (Gly-118, Gly-119) and the alkoxy pocket (Trp-84, Phe-330, Phe-331) that includes the anionic subsite residue Trp-84 (see Refs. 9 and 38 for a description of these sites). The extensive contacts were mainly participated by constituents of the pyran and the terpenoid moiety of TRB, as in this predicted TRB·AChE complex the inhibitor inserted its main body (tail) into the gorge while

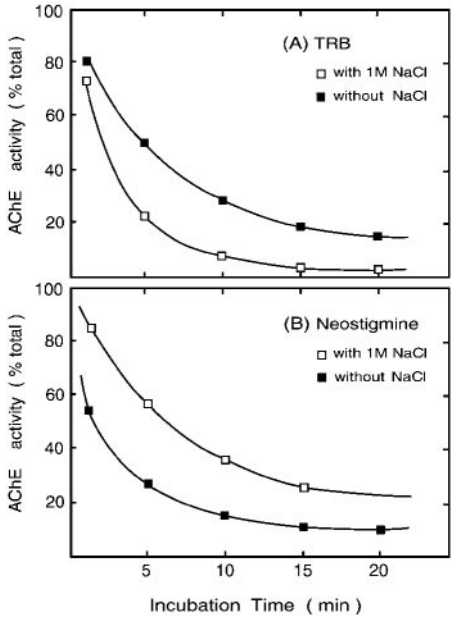

FIG. 5. **Inhibition of AChE by TRB or neostigmine in the presence or absence of 1 M NaCl.** The working AChE solution was incubated with the inhibitor, TRB or neostigmine, in the presence (*empty square*) or absence (*filled square*) of 1 M NaCl. At the indicated incubation times, enzyme activity was measured. The activity of a control assay in which no inhibitor was present in the enzyme solution was used as the denominator to calculate the percent of AChE activity of the inhibitor-incubated solutions. *A*, inhibition by TRB. *B*, inhibition by neostigmine.

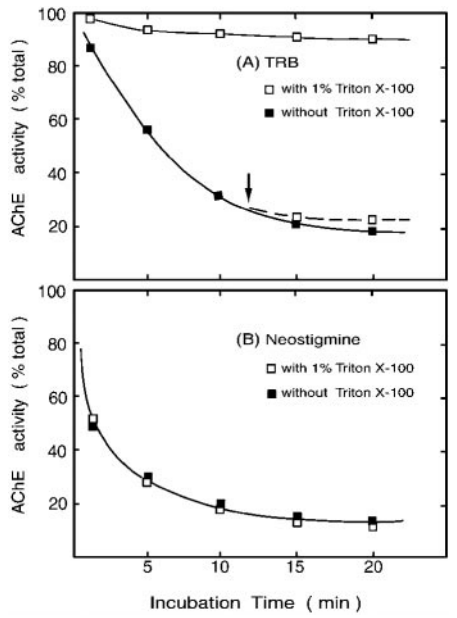

FIG. 6. **Inhibition of AChE by TRB or neostigmine in the presence or absence of Triton X-100.** The working AChE solution was incubated with the inhibitor, TRB or neostigmine, in the presence (*empty square*) or absence (*filled square*) of 1% Triton X-100. At the indicated incubation times, enzyme activity was measured. The activity of a control assay in which no inhibitor was present in the enzyme solution was used as the denominator to calculate the percent of AChE activity of the inhibitor-incubated solutions. *A*, inhibition by TRB. An *arrow* indicates when Triton X-100 was added during a post-incubation experiment. *B*, inhibition by neostigmine.

its head group protruded from the entrance of the gorge. Two amino acids, Tyr-121 and Ser-122, respectively, formed a hydrogen bond with the two hydroxyl groups (at positions 12a and 4a, Fig. 1) of TRB. Interestingly, several amino acids surrounding the rim of the gorge (Glu-73, Gln-74, Tyr-121, Phe-334, Ile-287, Trp-279) appeared to cramp TRB around the connecting bridge of its head and tail groups (Fig. 9*A*). This cramping may have prevented the inhibitor from entering further into the gorge (the inhibitor was at some distance from the catalytic site (6.8 Å from Ser-200), whereby a void near the bottom of the gorge was created (Fig. 9*A*)). To accommodate TRB in the gorge, a number of aromatic residues adopted a side chain conformation differing from those observed in presently available x-ray structures of AChE (Fig. 9*B*). The predicted side chain conformations were, however, energetically allowable, as indicated by an analysis with PROCHECK (Ref. 33; results not shown). There was also a notable shift in the cysteine loop, and this conformational shift contributed to contract the gorge entrance somewhat (Fig. 9*B*).

After completing the present modeling work, a crystal struc-

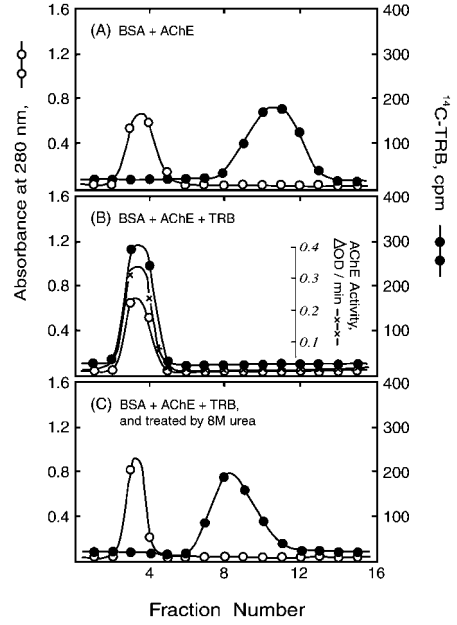

FIG. 7. **Effect of 8 M urea on the binding of [^{14}C]TRB to eel AChE.** The three specimens for experiments *A*, *B*, and *C* were prepared as described under "Experimental Procedures." These specimens were placed on a G-50 column, and effluents of 0.5 ml each were collected. UV absorption and radioactivity were measured for each effluent; for experiment *B*, AChE activity was also assayed. *BSA*, bovine serum albumin.

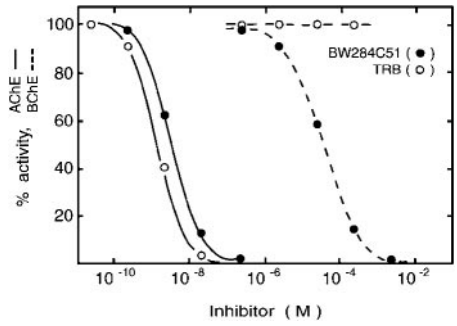

FIG. 8. **Dose-response inhibition of AChE and BChE by TRB or BW284C51.** The working enzyme solution was preincubated with the indicated inhibitor for 20 min at 25 °C before 5,5′-dithiobis(2-nitrobenzoic acid) and acetylthiocholine or butyrylthiocholine were added. Enzyme activity assays were then carried out. The enzyme activity of a control experiment in which the inhibitor was replaced by the same amount of methanol was regarded as 100% activity. The enzyme activities of the inhibitor-incubated solutions were compared with this 100% activity of the control. *Ordinate*, percent of enzyme activity relative to the control experiment. *Abscissa*, the final concentration of the inhibitor at the indicated period of preincubation.

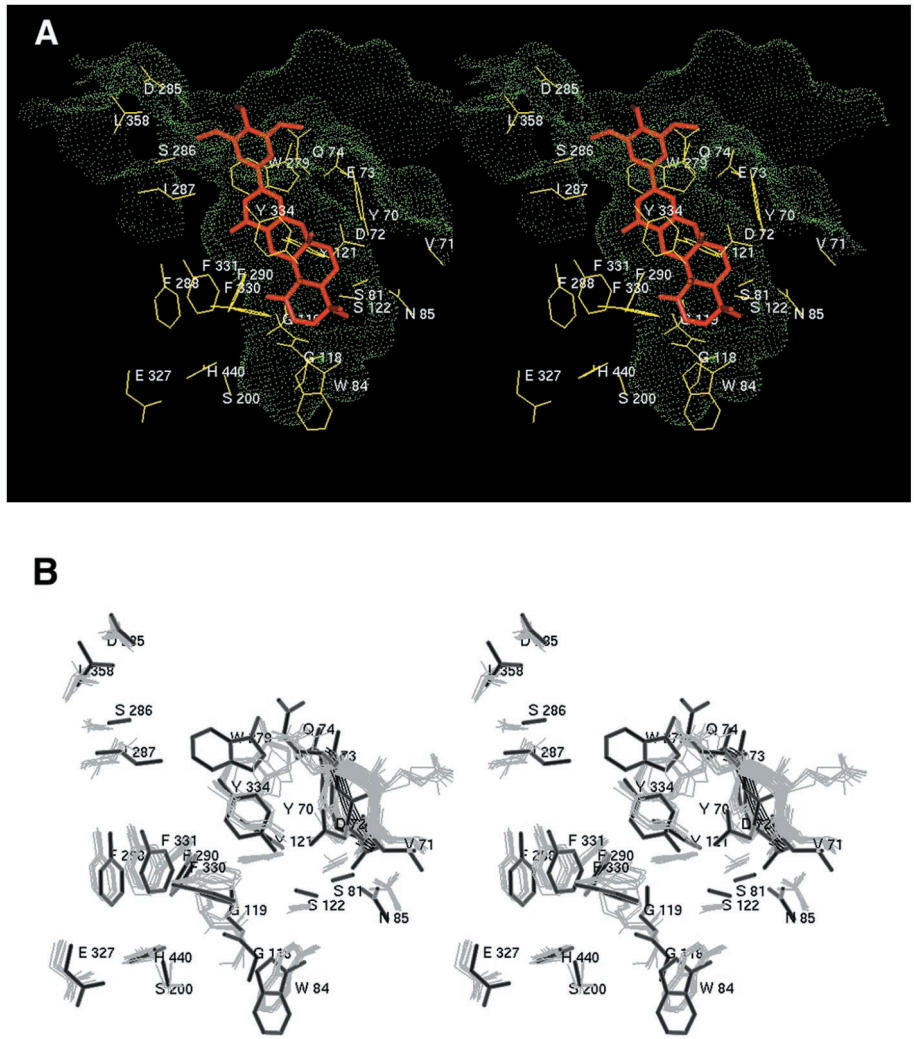

FIG. 9. **Stereo diagrams of the predicted TRB·AChE complex structure.** *A*, the catalytic triad (Ser-200, Glu-327, His-440) and the 23 amino acids that interact (heavy atom–heavy atom distance < 5Å, see text) with TRB (in *red*). The molecular surface that defines the gorge lumen (*green dots*) was created with a sphere probe of a 1.4-Å radius. *B*, a comparison between eight x-ray structures (Protein Data Bank codes 2ACE, 1ACJ, 1ACK, 1ACL, 1AMN, 1AX9, 1EVE, 1VOT; in *gray*) and the model (in *black*) on the side chain conformations of the catalytic triad and TRB-interacting amino acids. *Ribbon representations* mark the portion of the cysteine loop, a segment comprising amino acids 70 to 74, whose conformation changed significantly from the x-ray structure to the simulation-predicted model.

ture of AChE in complex with a new Alzheimer's drug known as E2020 was reported (39). E2020 is a long molecule consisting of three ring fragments, dimethoxyindanone, piperidine, and benzene, that are interposed by methylene groups. A comparison between our predicted model of TRB·AChE and the x-ray structure of E2020-AChE showed a considerably overlapped binding area, but the two differ in that TRB extrudes its trimethoxybenzyl group just out of the gorge entrance, whereas E2020 inserts its benzene ring very deep into the gorge, albeit still not directly contacting the active-site serine (39).

DISCUSSION

In our previous study of TRB inhibition on AChE extracted from the head of *Helicoverpa zea*, we observed an irreversible-like inhibition (13). We also reported that although dialysis or dilution recovers the activity of BW284C51-inhibited eel AChE, the same treatment has no effect on TRB-inhibited eel AChE (14). In the present kinetic investigation, we reaffirmed these earlier observations of irreversible AChE inhibition by using very diluted TRB during the preincubation period (Fig. 2). The use of nM concentrations TRB instead of μM concentrations of an earlier study (14) eliminated the possibility that TRB inhibits AChE via a noncompetitive inhibitory effect due to high inhibitor concentrations.

Covalent modification of active serine is the common mechanism that underlies the inhibition of serine proteases by substituted isocoumarins (40, 41) and, likewise, the inhibition of AChE by carbamates and organophosphates (9, 10). Because the structure of TRB contains an isocoumarin moiety, it would appear that TRB acts on AChE via a similar mechanism to exert its irreversible inhibition. However, although attractive intuitively, this explanation runs against several lines of experimental evidence. First, TRB does not inhibit serine proteases such as trypsin or chymotrypsin.[2] Second, TRB-inhibited eel AChE cannot be reactivated by a deacetylation agent (Fig. 4). Third, when treated with NaCl or Triton X-100, a drastically different inhibition time course was observed between TRB and neostigmine, the latter being an irreversible AChE inhibitor typical of those that form a covalent bond with the active serine of the enzyme. A high concentration of NaCl enhanced the inhibition for TRB, but the opposite was observed for neostigmine (Fig. 5). In contrast, preincubated Triton X-100 essentially abolished the inhibitory activities of TRB but had no effect on the inhibition of neostigmine (Fig. 6). These results may indicate that unlike neostigmine, whose reaction with AChE is thought to be guided initially by charge-charge interactions (42), the binding between TRB and AChE is mainly facilitated by hydrophobic interactions. This hydrophobic notion is consistent with the chemical structure of TRB (Fig. 1) and its lack of solubility at a moderate concentration (millimolar) as well as with the observation from gel filtration chromatography that TRB formed an aggregate with Triton X-100.[2] It appeared that the formation of the aggregate, which was absent

[2] J.-W. Chen and K.-H. Ling, unpublished observation.

in the case of neostigmine, allowed Triton X-100 to protect free AChE from TRB inhibition (Fig. 6). Furthermore, the fact that post-added Triton X-100 failed to rescue TRB-inhibited AChE (Fig. 6) suggests a tight binding between TRB and AChE, in agreement with the kinetic parameters deduced (Fig. 2).

An alternative mechanism is that, as has been suggested for onchidal (18), a novel covalent bond not with the active-site serine may be formed between TRB and the enzyme. Onchidal is a novel AChE inhibitor whose irreversible inhibition, like that of TRB, does not respond to oxime reactivators. However, TRB and onchidal are quite distinct from each other in terms of structure and size. In addition, onchidal possesses a potentially reactive α,β-unsaturated aldehyde by which the novel action of the inhibitor is implicated (18), and this unsaturated aldehyde functionality is lacking in TRB. More significantly, the fact that AChE-bound TRB can be released by 8 M urea (Fig. 7*C*) is strong evidence of noncovalent binding.

Taken together, our various findings led us to conclude that the inhibition of TRB on AChE is mediated by a tight noncovalent binding that is kinetically irreversible, at least within the time duration of our experiments. How could such a novel mechanism of AChE inhibition be attained? Our computer model predicted that TRB would act on the active gorge of the enzyme in such an unusual way that once TRB entered the gorge, it would somehow physically stick in the gorge to render an apparent irreversible noncovalent binding. Although there is not yet any direct evidence to verify our model at present, there is considerable indirect evidence to indicate that the following model is probable.

(*a*) The one-to-one stoichiometry (Fig. 3), high affinity (Fig. 2), and hydrophobic nature (Figs. 5 and 6) of the binding all favor the proposition that TRB acts on the active gorge of the enzyme. This proposition is also in line with the fact that all of the presently known and well characterized AChE inhibitors exert their inhibitory activity by binding to a part or parts (subsites) of the gorge (9, 10).

(*b*) Whereas the main members of the territrem family (TRA, TRB, TRC, and arisugacin A and B, which differ in their substituents to the benzyl group; Fig. 1*A*) display very similar AChE-inhibiting potency (14–16), modifications at the other end (tail) of the molecule often result in greatly reduced or even completely abolished inhibition (14).[3] For example, like TRB, TRC-benzyl (Fig. 1*A*) completely inhibits AChE at submicromolar concentrations; at the same concentration, MB2-succinate (see Fig. 1*A*) inhibits only up to 50% of the enzyme activity.[3] These data are consistent with a tail-in insertional orientation of TRB whereby its head, the benzyl group, protrudes from the gorge entrance, where there is an open space to accommodate a large structural group (Fig. 9*A*). A tail-in-inserted TRB to inhibit AChE is also in line with the modest and selective anti-AChE activities exhibited by some dihydroxanthone derivatives that are constructed based on the multi-ring part (tail) of the arisugacin (territrem) structure (43).

(*c*) By traversing almost the entire gorge and saving only a small portion at the bottom near the catalytic triad (Fig. 9*A*), TRB can make contacts with many gorge-lining aromatic residues, including those (Phe-288, Phe-290, Tyr-70, Tyr-121, Trp-279) that are present in AChE but absent in BChE. Interacting with these AChE-specific aromatic amino acids could explain the AChE selectivity of TRB and close analogs (Ref. 16; Fig. 8). Mutagenesis experiments involving other AChE-selective inhibitors (44, 45) support this line of explanation.

(*d*) In an assay to investigate whether TRB binds to acylated AChE, it was found that when [^{14}C]TRB was applied after the enzyme had been saturated with [^{3}H]DFP, [^{14}C]TRB still bound to the enzyme, whereas when [^{14}C]TRB was applied first, little binding of [^{3}H]DFP was observed (data not shown). That TRB is able to bind acylated AChE is consistent with the prediction that a void near the catalytic triad would be created upon TRB binding to the gorge (Fig. 9*A*), and this void is large enough to accommodate an AChE-linked DFP (verified by volume calculations; data not shown). Perhaps similarly, by not directly contacting the catalytic site, E2020 can also bind acylated AChE (39, 46). That DFP is no longer able to bind TRB-inhibited AChE suggests that TRB blocks not only the main entrance of the gorge but also the hypothetical back door or side wall entrance (5, 7). By inserting deep into the gorge with a tight, irreversible binding that involves multiple binding sites and the characteristic surface loop of the lipase/esterase superfamily (36, 37), TRB could significantly affect the conformational signal transduction pathway suggested by Shafferman and co-workers (37) and Shafferman *et al.* (47). A significant alteration of this pathway may prevent an alternative entrance to the active site from forming. In contrast, fasciculin, a powerful AChE inhibitor of 61 amino acids from the venom of mamba snakes, binds on the top of the gorge but does not enter it (48, 49), and perhaps as a consequence, a small agent like DFP can still reach the active-site serine via an alternative passage (Ref. 48 and references therein).

(*e*) Studies using molecular dynamics simulations (6, 8) have demonstrated the likelihood of a conformational gate located in a constricted area below the expanding opening of the gorge entrance. In our model, TRB positioned its bridging, narrowing neck near this structural gate and made extensive contacts with a number of residues (Tyr-121, Phe-290, Phe-330, Phe-331, Tyr-334; Fig. 9*A*) that are proposed to control the opening and closing of the gate. Therefore, it is conceivable that the entry of TRB, a unique AChE inhibitor that embodies a number of rigid ring structures with extruding methyl groups (Fig. 1), is facilitated by breathing motions of the conformational gate, and once TRB passes the gate, it is kinetically captured within the gorge. This is presumably because the gate, after being stuffed by the bulky and branching TRB, is no longer able to reopen to release the inhibitor. It is also possible that the gate is rigidified in a semi-open state, and the rigidification correlates with the predicted conformational change of the cysteine loop (Fig. 9*B*).

A significant number of mechanisms have been shown to be utilized by naturally occurring as well as synthesized compounds to inhibit AChE (9, 10). The present binding and inhibition assays of eel AChE with TRB, with augmented interpretations from molecular modeling results, revealed yet another novel mechanism of AChE inhibition. Kinetically irreversible or very slowly dissociating but noncovalent inhibition of AChE has been shown for fasciculin (50) and for an alkylpyridinium polymer (51). However, because it is considerably smaller than the two biopolymers and capable of entering deep into the gorge, TRB represents a unique variation of the noncovalent irreversible AChE inhibitors. The present work provides a framework for designing a new class of TRB-like inhibitors to further exploit the unusual gorge structure of AChE.

Acknowledgments—We thank Dr. Kenneth K. Wu for helpful discussions and reading the manuscript, Dr. W. S. Tzou and Edward S. C. Shih for technical assistance in modeling computations, and Douglas Pratt for editing the English.

REFERENCES

1. Barnard, E. A. (1974) in *The Peripheral Nervous System* (Hubbard, J. I., ed) pp. 201–204, Plenum Publishing Corp., New York
2. Quinn, D. M. (1987) *Chem. Rev.* **87,** 955–979
3. Sussman, J. L., Harel, M., Frolow, F., Oefner, C., Goldman, A., Toker, L., and Silman, I. (1991) *Science* **253,** 872–879
4. Ripoll, D. R., Faerman, C. H., Axelsen, P. H., Silman, I., and Sussman, J. L.

[3] H.-J. Pan and K.-H. Ling, unpublished data.

(1993) *Proc. Natl. Acad. Sci. U. S. A.* **90,** 5128–5132
5. Gilson, M. K., Straatsma, T. P., McCammon, J. A., Ripoll, D. R., Faerman, C. H., Axelsen, P. H., Silman, I., and Sussman, J. L. (1994) *Science* **263,** 1276–1278
6. Wlodek, S. T., Clark, T. W., Scott, L. R., and McCammon, J. A. (1997) *J. Am. Chem. Soc.* **119,** 9513–9522
7. Enyedy, I. J., Kovach, I. M., and Brooks, B. R. (1998) *J. Am. Chem. Soc.* **120,** 8043–8050
8. Zhou, H. X., Wlodek, S. T., and McCammon, J. A. (1998) *Proc. Natl. Acad. Sci. U. S. A.* **95,** 9280–9283
9. Taylor, P., and Radic, Z. (1994) *Annu. Rev. Pharmacol. Toxicol.* **34,** 281–320
10. Taylor, P. (1998) *Neurology* **51,** Suppl. 1, 830–835
11. Ling, K. H. (1994) *J. Toxicol. Toxin Rev.* **13,** 243–252
12. Arvanov, V. L., Ling, K. H., Chen, R. C., and Tsai, M. C. (1993) *Neurosci. Lett.* **152,** 69–71
13. Dowd, P. F., Peng, F. C., Chen, J. W., and Ling, K. H. (1992) *Entomol. Exp. Appl.* **65,** 57–64
14. Chen, J. W., and Ling, K. H. (1996) *J. Biomed. Sci.* **3,** 54–58
15. Omura, S., Kuno, F., Otoguro, K, Sunazuka, T., Shiomi, K., Masuma, R., and Iwai, Y. (1995) *J. Antibiot.* (*Tokyo*) **48,** 745–746
16. Otoguro, K., Kuno, F., and Omura, S. (1997) *Pharmacol. Ther.* **76,** 45–54
17. Lee, S. S., Peng, F. C., Chiou, C. M., and Ling, K. H. (1992) *J. Nat. Prod.* (*Lloydia*) **55,** 251–255
18. Abramson, S. N., Radic, Z., Manker, D., Faulkner, D. J., and Taylor, P. (1989) *Mol. Pharmacol.* **36,** 349–354
19. Ling, K. H., Yang, C. K., Kuo, C. A., and Kuo, M. D. (1982) *Appl. Environ. Microbiol.* **44,** 860–863
20. Ling, K. H., Liou, H. H., Yang, C. M., and Yang, C. K. (1984) *Appl. Environ. Microbiol.* **47,** 98–100
21. Peng, F. C., Ling, K. H., Wang, Y., and Lee, G. H. (1985) *Appl. Environ. Microbiol.* **49,** 721–723
22. Ling, K. H., Yang, C. K., and Huang, H. C. (1979) *Appl. Environ. Microbiol.* **37,** 358–361
23. Ling, K. H., Chang, M. F., Tsai, S. C., Peng, Y. W., Chen, B. J., and Wang, E. C. (1987) *Mycotoxin Res.* **3,** 7–12
24. Ling, K. H., Chiou, C. M., and Tseng, Y. L. (1991) *Drug Metab. Dispos.* **19,** 587–595
25. Ellman, G. L., Gourtney, K. D., Andres, V., Jr., and Featherstone, R. M. (1961) *Biochem. Pharmacol.* **7,** 88–95
26. Gordon, M. A., Carpenter, D. E., and Willson, J. B. (1978) *Mol. Pharmacol.* **14,** 266–270
27. Lowry, O. H., Rosebrough, N. J., Farr, A. L., and Randall, R. J. (1951) *J. Biol. Chem.* **193,** 265–275
28. Fox, B. W. (1968) *Int. J. Appl. Radiat. Isotopes* **19,** 717–730
29. Kitz, R., and Wilson, I. B. (1962) *J. Biol. Chem.* **237,** 3245–3249
30. Hsu, T. H., Yang, C. K., Ling, K. H., Wang, C. J., and Tang, C. P. (1982) *Crystallogr. Struct. Commun.* **11,** 199–206
31. Harel, M., Quinn, D. M, Nair, H. K., Silman, I., and Sussman, J. L. (1996) *J. Am. Chem. Soc.* **118,** 2340–2346
32. Antosiewicz, J., McCammon, J. A., Wlodek, S. T., and Gilson, M. K. (1995) *Biochemistry* **34,** 4211–4219
33. Laskowski, R. A., MacArthur, M. W., Moss, D. S., and Thornton, J. M. (1993) *J. Appl. Crystallogr.* **26,** 283–291
34. Raves, M. L., Harel, M., Pang, Y. P., Silman, I., Kozikowski, A. P., and Sussman, J. L. (1997) *Nat. Struct. Biol.* **4,** 57–63
35. Ding, H. Q., Karasawa, N., and Goddard, W, A., III (1992) *J. Chem. Phys.* **97,** 4309–4315
36. Cygler, M., Schrag, J. L., Harel, M., Silman, I., Gentry, M. K., and Doctor, B. P. (1993) *Protein Sci.* **2,** 366–382
37. Barak, D., Ordentlich, A., Bromberg, A., Kronman, C., Marcus, D., Lazar, A., Ariel, N., Velan, B., and Shafferman, A. (1995) *Biochemistry* **34,** 15444–15452
38. Ordentlich, A., Barak, D., Kronman, C., Ariel, N., Segall, Y., Velan, B., and Shafferman, A. (1996) *J. Biol. Chem.* **271,** 11953–11962
39. Kryger, G., Silman, I., and Sussman, J. L. (1999) *Structure* (*Lond.*) **7,** 297–307
40. Harper, J. W., Hemmi, K., and Powers, J. C. (1985) *Biochemistry* **24,** 1831–1841
41. Harper, J. W., and Powers, J. C. (1985) *Biochemistry* **24,** 7200–7213
42. Iverson, F., and Main, A. R. (1969) *Biochemistry* **8,** 1889–1895
43. Degen, S. J., Mueller, K. L., Shen, H. C., Mulder, J. A., Golding, G. M., Wei, L.-L., Zificsak, C. A., Neeno-Eckwall, A., and Hsung, R.-P. (1999) *Bioorg. Med. Chem. Lett.* **9,** 973–978
44. Harel, M., Sussman, J. L., Krejci, E., Bon, S., Chanal, P., Massoulie, J., and Silman, I. (1992) *Proc. Natl. Acad. Sci. U. S. A.* **89,** 10827–10831
45. Radic, Z., Pickering, N. A., Vellom, D. C., Camp, S., and Taylor, P. (1993) *Biochemistry* **32,** 12074–12084
46. Nochi, S., Asakawa, N., and Sato, T. (1995) *Biol. Pharm. Bull.* **18,** 1145–1147
47. Shafferman, A., Velan, B., Ordentlich, A., Kronman, C., Grosfeld, H., Leitner, M., Flashner, Y., Cohan, S., Barak, D., and Ariel, N. (1992) *EMBO J.* **11,** 3561–3568
48. Bourne, Y., Taylor, P., and Marchot, P. (1995) *Cell* **83,** 503–512
49. Harel, M., Kleywegt, G. J., Ravelli, R. B. G., Silman, I., and Sussman, J. L. (1995) *Structure* (*Lond.*) **3,** 1355–1366
50. Cervenansky, C., Dajas, F., Harvey, A. L., and Karlsson, E. (1991) in *Snake Toxins* (Harvey, A. L., ed) pp. 303–321, Pergamon Press Inc., New York
51. Sepcic, K., Marcel, V., Klaebe, A., Turk, T., Suput, D., and Fournier, D. (1998) *Biochim. Biophys. Acta* **1387,** 217–225
52. Tung, S.-S., Ling, K.-H., Tsai, S.-E., Chung, C.-H., Wang, J.-J., and Tung, T.-C. (1971) *J. Formosan Med. Assoc.* **70,** 251–257